Theoretical study on the reactions of (CF3)2CFOCH3 + OH/Cl and reaction of (CF3)2CFOCHO with Cl atom

ARTICLE *in* THE JOURNAL OF PHYSICAL CHEMISTRY A · JANUARY 2015

Impact Factor: 2.69 · DOI: 10.1021/jp5125553 · Source: PubMed

6 AUTHORS, INCLUDING:

Feng-Yang Bai
Northeast Normal University
5 PUBLICATIONS **4** CITATIONS

SEE PROFILE

Xiu-Mei Pan
Northeast Normal University
93 PUBLICATIONS **720** CITATIONS

SEE PROFILE

THE JOURNAL OF PHYSICAL CHEMISTRY A

Article

pubs.acs.org/JPCA

Theoretical Study on the Reactions of $(CF_3)_2CFOCH_3$ + OH/Cl and Reaction of $(CF_3)_2CFOCHO$ with Cl Atom

Feng-Yang Bai,[†] Gang Sun,[‡] Xu Wang,[†] Yan-Qiu Sun,[†] Rong-Shun Wang,[†] and Xiu-Mei Pan*[,†]

[†]Institute of Functional Material Chemistry, Faculty of Chemistry, Northeast Normal University, 130024 Changchun, People's Republic of China

[‡]Department of Chemistry and Biology, Bei Hua University, 132013 Jilin, People's Republic of China

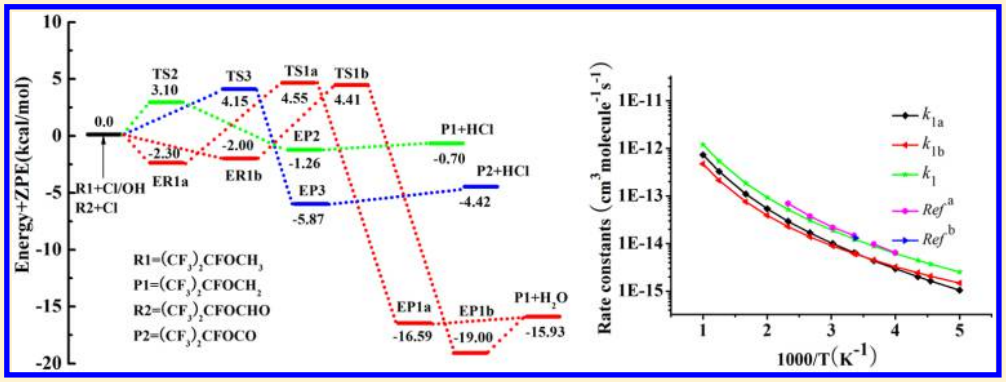

ABSTRACT: Reactions of $(CF_3)_2CFOCH_3$ and $(CF_3)_2CFOCHO$ with hydroxyl radical and chlorine atom are studied at the B3LYP and BHandHLYP/6-311+G(d,p) levels along with the geometries and frequencies of all stationary points. This study is further refined by CCSD(T) and QCISD(T)/6-311+G(d,p) methods in the minimum energy paths. For the reaction $(CF_3)_2CFOCH_3$ + OH, two hydrogen abstraction channels are found. The total rate constants for the reactions $(CF_3)_2CFOCH_3$ + OH/Cl and $(CF_3)_2CFOCHO$ + Cl are followed by means of the canonical variational transition state with the small-curvature tunneling correction. The comparison between the hydrogen abstraction rate constants by hydroxyl and chlorine atom is discussed. Calculated rate constants are in reasonable agreement with the available experiment data. The standard enthalpies of formation for the reactants, $(CF_3)_2CFOCH_3$ and $(CF_3)_2CFOCHO$, and two products, $(CF_3)_2CFOCH_2$ and $(CF_3)_2CFOCO$, are evaluated by a series of isodesmic reactions. The Arrhenius expressions for the title reactions are given as follows: $k_1 = 1.08 \times 10^{-22} T^{3.38} \exp(-213.31/T)$, $k_2 = 3.55 \times 10^{-22} T^{3.61} \exp(-240.26/T)$, and $k_3 = 3.00 \times 10^{-19} T^{2.58} \exp(-1294.34/T)$ cm^3 $molecule^{-1}$ s^{-1}.

1. INTRODUCTION

The increase of atmospheric concentration of halogenated organic compounds is partially responsible for the change in the global climate.[1,2] Some halogenated ethers or hydrofluoroethers (HFEs) such as methyl perfluoroisopropyl ether ($(CF_3)_2CFOCH_3$) are widely used in different industries.[3,4] There is an ether linkage −O− in $(CF_3)_2CFOCH_3$, which is expected to increase its reactivity and decrease its atmospheric lifetime.[5−7] Numerous C−F bonds of halogenated ethers may absorb infrared radiation[8] and contribute to global warming. A detailed knowledge of the atmospheric chemistry of the HFEs is needed to assess the environmental impact of these compounds prior to their large-scale industrial use. $(CF_3)_2CFOCH_3$ is a classical specie of HFEs; it does not contain chlorine and therefore will not contribute to the well-established chlorine-based catalytic destruction of stratospheric-ozone.[9] $(CF_3)_2CFOCHO$ is an important class of volatile organic compounds (VOCs). The −CHO in $(CF_3)_2CFOCHO$ is directly discharged into the troposphere from biogenic and anthropogenic sources[10] and has received regulatory attention because of its potential adverse health effects on humans as well as its important role in atmospheric photochemical reactions. As for an oxidative product of $(CF_3)_2CFOCH_3$, $(CF_3)_2CFOCHO$ also has some chemical properties similar to those of $(CF_3)_2CFOCH_3$. For example, $(CF_3)_2CFOCH_3$ and $(CF_3)_2CFOCHO$ contain C−H bond, which can be oxidized by hydroxyl radical or chlorine atom. Reactions with the highly reactive radicals are important for evaluating the atmospheric lifetime of $(CF_3)_2CFOCH_3$ and $(CF_3)_2CFOCHO$ in the stratosphere.[11−13] Tokuhashi et al.[14] have reported the rate constants of $(CF_3)_2CFOCH_3$ + OH using flash photolysis, laser photolysis, and discharge flow methods combined with laser-induced fluorescence technique at the temperature range of 250−430 K. The Arrhenus expression was determined to be $k_{(CF_3)_2CFOCH_3+OH} = (1.94^{+0.48}_{-0.38} \times 10^{-12} \exp[-(1450 \pm 70)/T])$. Recently, Andersen et al.[9] studied the hydrogen abstraction

Received: December 16, 2014
Revised: January 28, 2015
Published: January 28, 2015

DOI: 10.1021/jp5125553
J. Phys. Chem. A 2015, 119, 1256−1266

reactions on the temperature dependence of the rate constants for the title reactions using Fourier transform infrared (FTIR) smog chamber techniques. The experimental rate constants were found to be $(1.55 \pm 0.24) \times 10^{-14}$ cm^3 molecule^{-1} s^{-1} for the reaction $(CF_3)_2CFOCH_3$ + OH, $(1.80 \pm 0.42) \times 10^{-13}$ cm^3 molecule^{-1} s^{-1} for $(CF_3)_2CFOCH_3$ + Cl, and $(1.47 \pm 0.56) \times 10^{-14}$ cm^3 molecule^{-1} s^{-1} for $(CF_3)_2CFOCHO$ + Cl at 296 ± 1 K. The experiment did not cover a wide temperature range of practical interest. As a result, theoretical studies on the accurate extrapolation of rate constants in higher temperatures for the title reactions are very necessary. No experimental information is available on the branching ratios of the rate constant of the reaction $(CF_3)_2CFOCH_3$ + OH; it is desirable to give a further understanding of the reaction mechanism and the dynamics content. Experimentally and theoretically, the mechanism of such reactions of halogenated ethers with various free radicals has been extensively studied and continues to receive considerable attention.[15−27] In this present work, we will focus attention on the reactions $(CF_3)_2CFOCH_3$ + OH/Cl and $(CF_3)_2CFOCHO$ with Cl atom. Because of the formation of a hydrogen bond between F atom of $(CF_3)_2CFOCH_3$ and H of OH radical, two H-abstraction channels are found for $(CF_3)_2CFOCH_3$ + OH reaction. However, only one H-abstraction channel is found for $(CF_3)_2CFOCH_3$ + Cl reaction.

$$(CF_3)_2CFOCH_3 + OH \rightarrow (CF_3)_2CFOCH_2 + H_2O \quad \text{(R1a,b)}$$

$$(CF_3)_2CFOCH_3 + Cl \rightarrow (CF_3)_2CFOCH_2 + HCl \quad \text{(R2)}$$

$$(CF_3)_2CFOCHO + Cl \rightarrow (CF_3)_2CFOCO + HCl \quad \text{(R3)}$$

As far as we know, there is no previous theoretical work for the set of these reactions. In the study, density functional theory (DFT) and high-level ab initio calculations are presented on the reaction mechanism of the title reactions, followed by dual-level direct dynamics studies for the rate constants over a wide temperature region of 200−1000 K. The electronic structure calculations provide the necessary information on the potential energy surface (PES) of the reaction system and extra points along the minimum energy paths (MEPs). The rate constants and product branching ratios are calculated by the variational transition state theory (VTST) with interpolated single-point energies (ISPE). In addition, a discussion of the comparison between the experiment and computation is provided.

2. METHODOLOGY

The equilibrium geometries and frequencies of the reactants, products, complexes, and transition states are optimized and calculated at Becke's three-parameter hybrid functional with local correlation functional of Lee−Yang−Par level of theory (B3LYP)[28,29] using the standard 6-311+G(d,p) basis set. The zero-point energy (ZPE) corrections are obtained at the same level of theory. The B3LYP method was widely accurate for predicting credible results in many articles.[30,31] The stationary nature of the structure is proved by harmonic vibrational frequency calculation. That is, the equilibrium species possess all real frequency, whereas transition states possess only one imaginary frequency. Intrinsic reaction coordinate (IRC)[32,33] calculations are performed to confirm that the transition state connects to the desired reactants and products at the B3LYP/6-311+G(d,p) level. To ensure the veracity of stationary points, the BHandHLYP/6-311+G(d,p)[28,29] level is also employed in optimizing the geometries. Furthermore, the energy profiles are further refined at the CCSD(T)/6-311+G(d,p)[34] and QCISD-(T)/6-311+G(d,p)[35] levels based on the B3LYP/6-311+G(d,p) geometries. The T_1-diagnostic is a qualitative measure of multireference character. The T_1 values of all species in our system are smaller than 0.045, indicating that multireference character in CCSD(T) wave function is not a problem.[36] All the electronic structures are carried out with Gaussian 09 program package.[37]

The initial PES information, including optimized geometries, energies, and frequencies along the MEPs as determined from IRC theory, are prepared for dynamic calculations. Rate constants are calculated over the wide temperature range of 200−1000 K using the canonical variational transition state theory (CVT)[38−40] involving small-curvature tunneling correction (SCT)[41,42] method proposed by Truhlar and co-workers. Canonical variational transition state theory rate constants, $k^{CVT}(T)$, at fixed temperature (T) by minimizing the generalized transition state theory rate constant, $k^{GT}(T,s)$, with respect to the dividing surface at s is expressed as

$$k_s^{CVT}(T) = \min k^{GT}(T, s)$$

where k^{GT} for temperature T and dividing surface at s is

$$k^{GT}(T, s) = \frac{\sigma Q^{GT}(T, s)}{\beta h Q^{R}(T)} \exp(-\beta V_{MEP}(s))$$

In this equation, s is the location of the generalized transition state on the IRC; σ is the symmetry factor; h is Planck's constant; β equals $(k_B T)^{-1}$ where k_B is Boltzmann's constant; Q^{GT} and Q^{R} are partition functions for the generalized transition state and reactants, respectively. In the calculations of the electronic partition functions, two electronic states for OH radical, with a 140 cm^{-1} splitting in the $^2\Pi$ ground state, are included. The two low-lying electronic states, $^2P_{1/2}$ and $^2P_{3/2}$, with a splitting of 881 cm^{-1} of Cl atom, are also included. To take tunneling effect into account, the CVT rate constant is multiplied by the small-curvature tunneling approximation, which is denoted as $k^{SCT/CVT}(T)$. All vibrational modes are treated quantum mechanically as harmonic oscillators except for the lowest vibrational mode. The dynamic calculations of the VTST with the ISPE (VTST-ISPE)[43] are carried out through the POLYRATE, version 9.7 program.[44]

Accurate enthalpies of formation ($\Delta H^{\theta}_{f,298}$) are important for the kinetic calculations. The isodesmic reaction is a convenient method for predicting the standard enthalpies of formation. The enthalpies of formation for species $(CF_3)_2CFOCH_3$, $(CF_3)_2CFOCH_2$, $(CF_3)_2CFOCHO$, and $(CF_3)_2CFOCO$ are predicted by the following isodesmic reactions.

$$(CF_3)_2CFOCH_3 + CH_4 + CH_3 \rightarrow CH_3OCH_3 + CF_3CH_3 + CHFCF_3 \quad \text{(R4a)}$$

$$(CF_3)_2CFOCH_3 + CH_4 + CF_3 \rightarrow CH_3OCH_3 + CF_3CF_3 + CHFCF_3 \quad \text{(R4b)}$$

$$(CF_3)_2CFOCH_3 + CH_4 + CH_3 \rightarrow CH_3OCH_3 + CF_3CH_2CH_3 + CH_3F \quad \text{(R4c)}$$

$$(CF_3)_2CFOCH_2 + CH_4 + CH_4 \rightarrow CH_3OCH_3 + CF_3CH_3 + CHFCF_3 \quad \text{(R5a)}$$

$$(CF_3)_2CFOCH_2 + CH_4 + CHF_3 \rightarrow CH_3OCH_3 + CF_3CF_3 + CHFCF_3 \quad \text{(R5b)}$$

DOI: 10.1021/jp5125553
J. Phys. Chem. A 2015, 119, 1256−1266

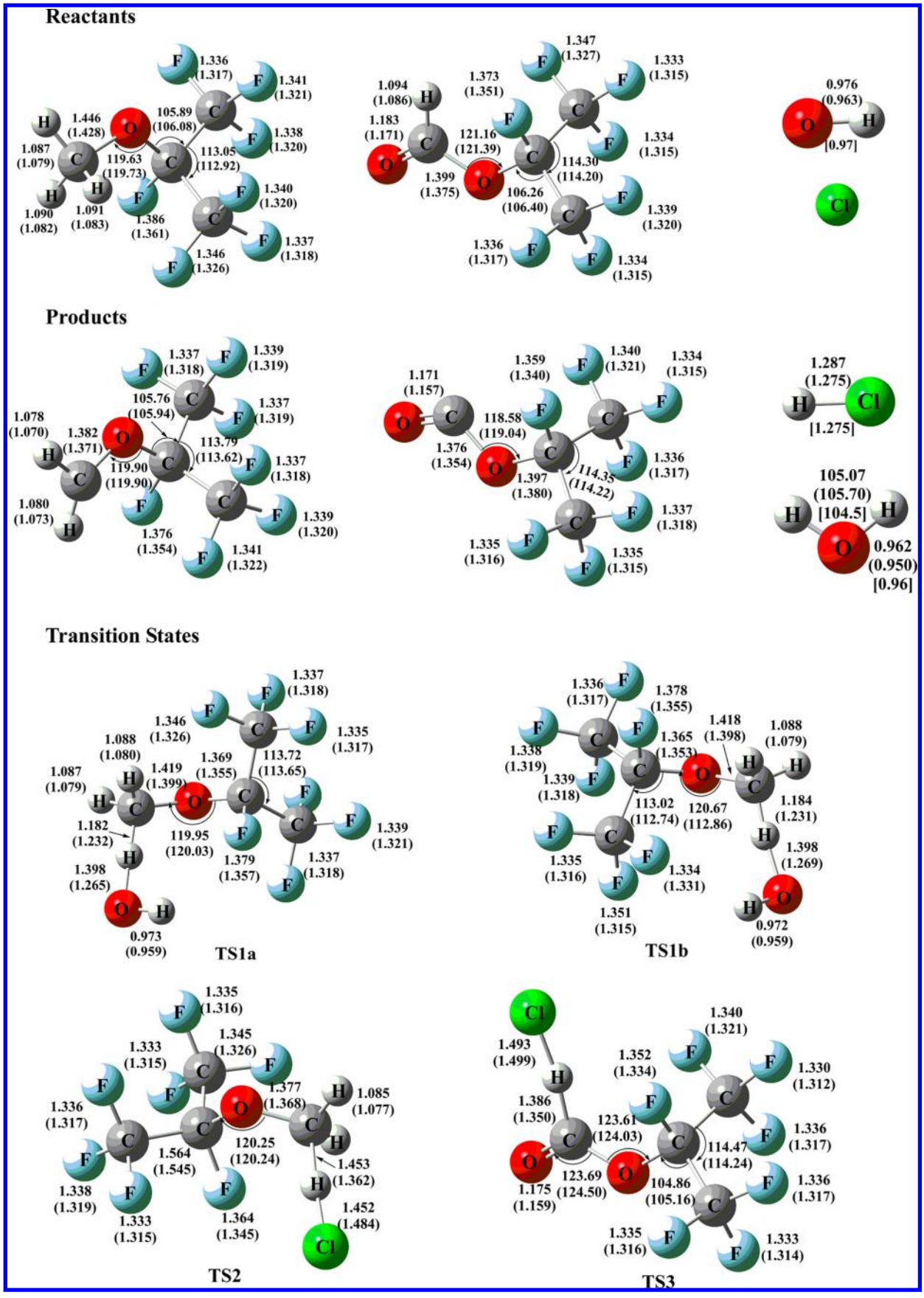

Figure 1. continued

DOI: 10.1021/jp5125553
J. Phys. Chem. A 2015, 119, 1256−1266

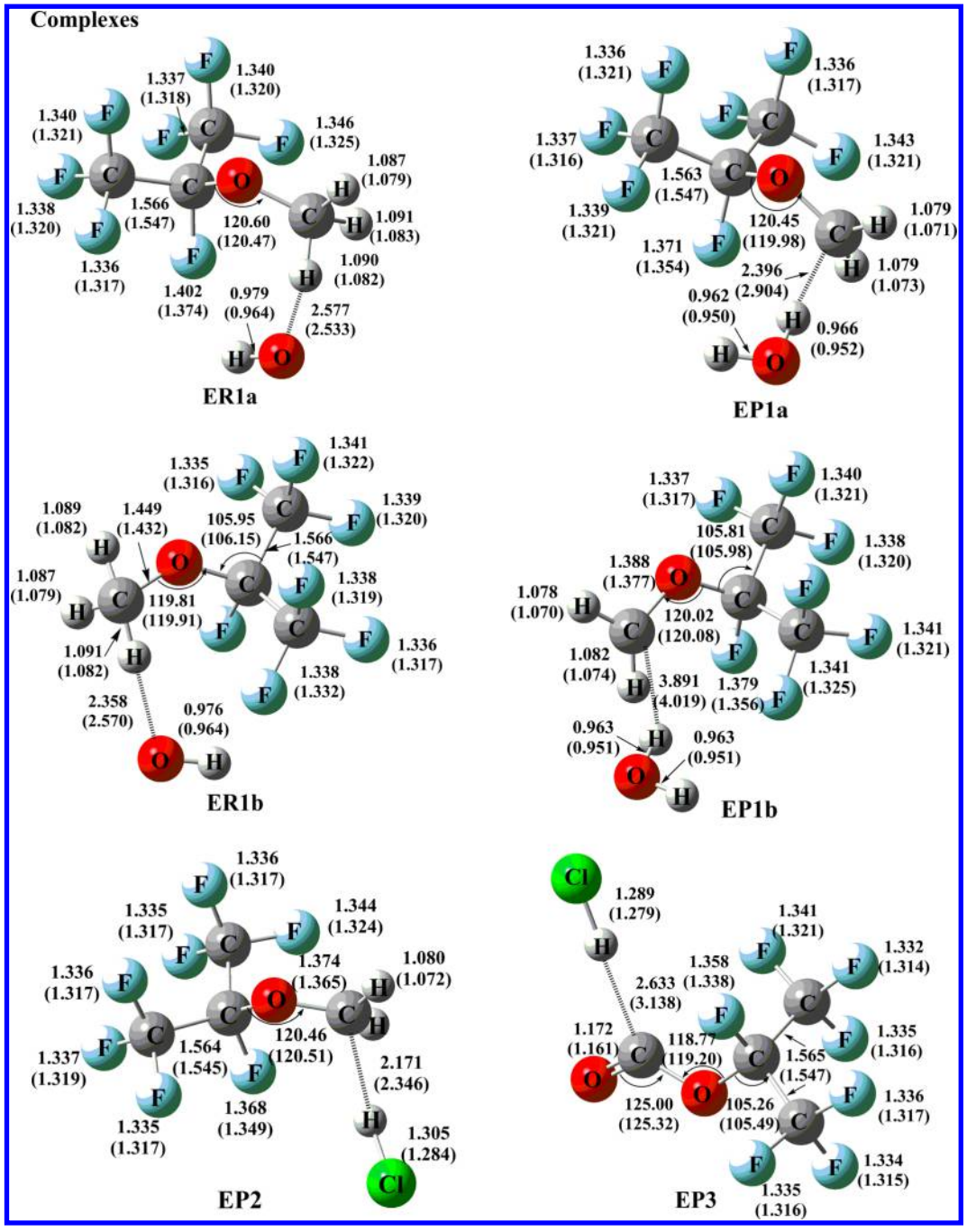

Figure 1. Optimized geometries of the reactants, products, transition states, and complexes at the B3LYP/6-311+G(d,p) and BHandHLYP/6-311+G(d,p) (in parentheses) levels and the limited experimental values (in square brackets). Bond lengths are in angstroms and angles in degrees.

$$(CF_3)_2CFOCH_2 + CH_4 + CH_3F + CH_4 \rightarrow CH_3OCH_3 + CF_3CH_2CH_3 + CH_2CF_2 + CH_3 \quad (R5c)$$

$$(CF_3)_2CFOCHO + CH_4 + CH_4 + CH_3 \rightarrow CH_3OCH_3 + CF_3CH_2CH_3 + CH_3F + CHO \quad (R6a)$$

$$(CF_3)_2CFOCHO + CH_4 + CH_4 + CH_3 \rightarrow CH_3OCH_3 + CF_3CH_3 + CHFCF_3 + CHO \quad (R6b)$$

$$(CF_3)_2CFOCHO + CH_4 + CH_3 + CF_3 \rightarrow CH_3OCH_3 + CF_3CF_3 + CHFCF_3 + CHO \quad (R6c)$$

$$(CF_3)_2CFOCO + CH_4 + CH_4 + CH_3F \rightarrow CH_3OCH_3 + CF_3CH_2CH_3 + CH_2F_2 + CHO \quad (R7a)$$

$$(CF_3)_2CFOCO + CH_4 + CH_4 + CH_3 \rightarrow CH_3OCH_3 + CF_3CH_3 + CHFCF_3 + CHO \quad (R7b)$$

$$(CF_3)_2CFOCO + CH_3 + CH_4 + CHF_3 \rightarrow CH_3OCH_3 + CF_3CF_3 + CHFCF_3 + CHO \quad (R7c)$$

It is well-known that the spin contamination can lead to imprecise values in the barrier height.[45,46] The spin contamination was examined before and after annihilation for the species related to the title reactions. The doublet range

DOI: 10.1021/jp5125553
J. Phys. Chem. A 2015, 119, 1256−1266

Table 1. Frequencies (Experimental Values Are in Parentheses) (cm^{-1}) and $\langle s^2 \rangle$ Values of the Reactants, Products, Transition States, and Hydrogen-Bonded Complexes for the Title Reactions Calculated at the B3LYP/6-311+G(d,p) Level

species	B3LYP/6-311+G(d,p)[a]	$\langle s^2 \rangle$
$(CF_3)_2CFOCH_3$	33, 64, 98, 153, 171, 192, 227, 267, 289, 309, 336, 366, 377, 449, 529, 545, 557, 595, 660, 725, 760, 966, 1002, 1066, 1145, 1163, 1171, 1178, 1208, 1215, 1229, 1291, 1331, 1483, 1498, 1502, 3055, 3137, 3163	0.0
$(CF_3)_2CFOCHO$	28, 66, 109, 154, 185, 207, 248, 266, 290, 308, 335, 371, 377, 448, 529, 546, 556, 569, 597, 664, 725, 763, 984, 1064, 1093, 1152, 1166, 1182, 1210, 1218, 1238, 1284, 1331, 1461, 3160, 3314	0.0
$(CF_3)_2CFOCH_2$	34, 61, 77, 137, 146, 166, 227, 255, 279, 307, 328, 348, 364, 416, 514, 529, 550, 557, 621, 719, 739, 814, 956, 1004, 1014, 1120, 1143, 1154, 1183, 1219, 1233, 1284, 1324, 1409, 1870, 3096	0.753
$(CF_3)_2CFOCO$	29, 59, 82, 139, 145, 183, 227, 248, 278, 307, 328, 348, 363, 416, 511, 529, 550, 558, 622, 718, 737, 803, 945, 1004, 1111, 1146, 1160, 1181, 1226, 1232, 1284, 1318, 1915	0.753
OH	3708 (3775)	0.752
H_2O	1602 (1595), 3818 (3657), 3923 (3756)	0.0
HCl	2928 (2991)	0.0
TS1a	465*i*, 25, 35, 51, 74, 136, 155, 172, 187, 230, 261, 281, 307, 329, 341, 356, 379, 446, 528, 548, 556, 594, 669, 721, 762, 770, 978, 1011, 1056, 1109, 1146, 1149, 1174, 1212, 1222, 1226, 1241, 1285, 1331, 1394, 1469, 1516, 3097, 3186, 3742	0.756
TS1b	468*i*, 29, 39, 65, 96, 142, 155, 181, 191, 230, 265, 286, 307, 327, 339, 376, 380, 448, 529, 547, 557, 595, 666, 723, 761, 785, 970, 983, 1024, 1090, 1142, 1145, 1176, 1208, 1213, 1229, 1248, 1286, 1328, 1383, 1472, 1555, 3094, 3180, 3748	0.756
TS2	686*i*, 28, 32, 36, 72, 114, 149, 188, 231, 265, 292, 307, 333, 355, 371, 408, 444, 528, 538, 556, 561, 598, 675, 722, 764, 942, 962, 983, 1059, 1124, 1155, 1175, 1181, 1186, 1223, 1231, 1248, 1284, 1330, 1469, 3111, 3237	0.755
TS3	1045*i*, 31, 37, 55, 63, 88, 139, 161, 224, 250, 268, 287, 305, 315, 335, 350, 363, 437, 529, 540, 552, 559, 633, 721, 741, 814, 868, 985, 1032, 1046, 1107, 1160, 1163, 1188, 1230, 1238, 1278, 1320, 1898	0.755
1ERa	11, 40, 50, 79, 82, 115, 156, 179, 201, 228, 246, 268, 289, 309, 326, 336, 365, 379, 449, 529, 542, 557, 594, 651, 725, 757, 957, 995, 1028, 1144, 1163, 1174, 1184, 1209, 1214, 1232, 1293, 1337, 1491, 1494, 1505, 3054, 3139, 3167, 3665	0.752
1ERb	19, 32, 40, 63, 69, 100, 144, 148, 154, 173, 203, 227, 266, 288, 307, 335, 365, 376, 449, 529, 545, 557, 595, 661, 725, 759, 959, 995, 1064, 1137, 1162, 1169, 1176, 1206, 1216, 1229, 1290, 1330, 1482, 1491, 1505, 3049, 3134, 3164, 3714	0.752
1EPa	12, 17, 31, 58, 78, 86, 117, 154, 160, 190, 202, 227, 265, 289, 307, 332, 340, 358, 383, 446, 528, 549, 557, 568, 595, 670, 723, 764, 981, 1063, 1104, 1152, 1173, 1184, 1208, 1224, 1243, 1284, 1333, 1462, 1611, 3164, 3318, 3753, 3889	0.753
1EPb	20, 25, 31, 42, 61, 103, 117, 155, 177, 183, 204, 228, 266, 289, 307, 320, 335, 371, 377, 448, 528, 545, 557, 594, 610, 663, 724, 762, 982, 1056, 1087, 1148, 1163, 1179, 1213, 1216, 1234, 1286, 1331, 1477, 1619, 3144, 3309, 3815, 3917	0.753
2EP	16, 20, 32, 51, 78, 126, 155, 186, 217, 250, 269, 292, 308, 334, 357, 374, 397, 440, 447, 528, 549, 557, 595, 670, 683, 723, 764, 982, 1065, 1111, 1154, 1173, 1186, 1211, 1225, 1246, 1283, 1331, 1461, 2640, 3152, 3302	0.753
3EP	8, 14, 26, 31, 58, 81, 128, 141, 142, 157, 218, 234, 248, 279, 307, 328, 348, 363, 416, 511, 529, 550, 558, 622, 718, 738, 804, 966, 1010, 1106, 1148, 1161, 1185, 1226, 1236, 1282, 1319, 1908, 2883	0.753

[a]Experimental values in parentheses are taken from ref 47.

from 0.752 to 0.756 before annihilation; nevertheless, the $\langle s^2 \rangle$ is 0.75 (the exact data for a pure doublet) after annihilation. Thus, the wave functions were not severely contaminated by states of higher multiplicity.

3. RESULTS AND DISCUSSION

3.1. Stationary Points and Reaction Mechanism. The optimized geometric parameters of the reactants, products, complexes, and transition states (TS1a, TS1b, TS2, and TS3) for the title reactions calculated at the B3LYP/6-311+G(d,p) and BHandHLYP/6-311+G(d,p) levels are presented in Figure 1, along with the offered experimental values. From Figure 1, it can be seen that the optimized parameters, obtained at the two levels, are reasonably consistent with each other. The computational parameters of OH, H_2O, and HCl are in good line with the corresponding experimental values.[47] At the B3LYP/6-311+G(d,p) level, the length of the breaking C−H bond in TS1a is 8.3% longer than the equilibrium C−H bond length in $(CF_3)_2CFOCH_3$. In addition, the forming bonds O−H is 45.3% longer than the corresponding equilibrium bond length of O−H bond in H_2O. The elongation of the forming bond is greater than that of the breaking bond, indicating that TS1a is a reactant-like barrier. This reaction channel will proceed via an early transition state. Similar result can be obtained in TS1b. We can see that the C−H bond in TS2 structure will be broken, increased by 33.2% compared with the C−H equilibrium bond length in $(CF_3)_2CFOCH_3$, and the forming H−Cl bond is about 12.8% longer than the regular bond length of HCl. In TS3, the breaking C−H bond is 26.7% longer than the equilibrium C−H bond length in $(CF_3)_2CFOCHO$. However, the forming H−Cl bond stretches by 16.0% over the equilibrium H−Cl bond length in HCl. The elongation of the breaking bond is larger than that of the forming bond, suggesting that TS2 and TS3 of the title reactions are both product-like barriers, i.e., both reaction channels will proceed via late transition states. The same results can be obtained at the BHandHLYP/6-311+G(d,p) level.

Table 1 gives the harmonic vibrational frequencies of the reactants, products, complexes, and transition states at the B3LYP/6-311+G(d,p) level as well as the corresponding experimental results.[47] The calculated frequencies of OH, H_2O, and HCl are in good agreement with the experimental values. Each transition state yields one and only one imaginary frequency corresponding to the stretching modes of the coupling breaking and forming bonds. The values of these imaginary frequencies are 465*i*, 468*i*, 686*i*, and 1045*i* for TS1a, TS1b, TS2, and TS3, respectively. Table 2 lists the relative energies (Er) with zero-point energy (ZPE) corrections of main species for the title reactions at the B3LYP/6-311+G(d,p), QCISD(T) and CCSD(T)//B3LYP/6-311+G(d,p) levels, respectively. Calculated results show that the values obtained at CCSD(T) and QCISD(T) levels are very close, with the largest deviation within a factor of 0.30 kcal/mol.

A schematic potential energy surface of the title reactions obtained at the QCISD(T)//B3LYP/6-311+G(d,p) level is described in Figure 2. Note that the energies of reactants are set to be zero for reference. For reaction channels R1a and R1b, the reactant complexes (ER1a, ER1b) are located at the entrance of the channels, respectively. The energies of ER1a and ER1b are lower than these reactants ($(CF_3)_2CFOCH_3$ and

DOI: 10.1021/jp5125553
J. Phys. Chem. A 2015, 119, 1256−1266

Table 2. Relative Energies (Er) of Main Species for Reactions R1−R3 at the B3LYP/6-311+G(d,p), CCSD(T)//B3LYP/6-311+G(d,p), and QCISD(T)//B3LYP/6-311+G(d,p) Levels (kcal/mol) with the ZPE Corrections (a.u.)

species	ZPE(B3LYP)	B3LYP	CCSD(T)//B3LYP	QCISD(T)//B3LYP
R1+OH	0.089379	0.00	0.00	0.00
1ERa	0.090971	−1.36	−2.28	−2.30
TS1a	0.087666	−0.49	4.76	4.55
1EPa	0.089245	−17.63	−16.48	−16.58
1ERb	0.090273	−1.07	1.99	−2.00
TS1b	0.087745	−0.71	4.64	4.41
EP1b	0.089401	−19.43	−18.90	−19.01
P1+ H_2O	0.087842	−17.51	−15.84	−15.93
R1+Cl	0.080929	0.00	0.00	0.00
TS2	0.074099	−2.11	3.24	3.10
2EP	0.075092	−3.37	−1.19	−1.26
P1+HCl	0.073224	−3.08	−0.66	−0.70
R2+Cl	0.062005	0.00	0.00	0.00
TS3	0.055428	−0.61	4.45	4.15
3EP	0.056968	−5.73	−5.65	−5.87
P2+HCl	0.056145	−5.78	−4.21	−4.42

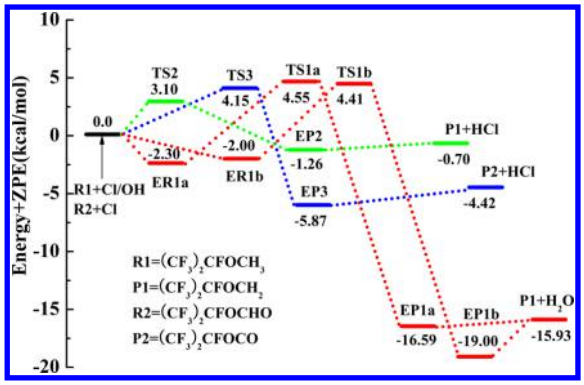

Figure 2. Schematic potential energy surfaces for the title reactions. Relative energies (in kilocalories per mole) are calculated at the QCISD(T)//B3LYP/6-311+G(d,p) + ZPE level.

OH) by 2.3 and 2.0 kcal/mol, respectively. Then, starting from the complexes, the reactions via two transition states TS1a and TS1b to form two complexes in the exit routes, which are about 0.66 and 3.07 kcal/mol lower than the products. With respect to channels R1a and R1b, the relative energy of TS1a (4.55 kcal/mol) is only 0.14 kcal/mol larger than that of TS1b (4.41 kcal/mol). Thus, these two reaction channels may be competitive over the whole temperature range. This view will be verified by the rate constant calculation in the following section. Devi and Chandra[15] have investigated the reaction of $(CF_3)_2CHOCH_3$ with OH radical theoretically, and the H-abstraction from $-CH_3$ group was found to be the dominated channel. The circumstance of PES is similar to our results. For reaction R2, the attack of Cl atom on the C−H bond of $(CF_3)_2CFOCH_3$ would proceed via TS2 with a 3.10 kcal/mol barrier. The whole reaction pathway is very similar to $(CF_3)_2CHOCH_2F$ with Cl atom. Singh et al.[16] have found that the barrier of the H-abstraction channel from the $-CH_2F$ group was 3.40 kcal/mol at the CCSDT/6-311G(d,p) level. The $(CF_3)_2CFOCH_3$ and $(CF_3)_2CHOCH_2F$ are isomers; the different site of F atoms can lead to different barrier values. Beyond that, the reaction of $(CF_3)_2CHOCH_2F$ with Cl atom in MEP also arrives at a situation similar to our results.[17] The barrier height of the reaction of $(CF_3)_2CFOCH_3$ with OH radical is higher than that of reaction with Cl atom. Thus, the rate of R2 will be faster than that of R1.[9] Similar to reaction R2, there exists a product complex (EP3), which lies 1.45 kcal/mol below the corresponding products at the exit of reaction $(CF_3)_2CFOCHO$ with Cl atom. This process needs to overcome the barrier with 4.15 kcal/mol energy. Comparing reaction $(CF_3)_2CFOCH_3$ + Cl with $(CF_3)_2CFOCHO$ + Cl, we can find that the barrier height is 1.05 kcal/mol lower than that of the latter, showing that the rate of R2 will also be faster than R3.[9]

3.2. Enthalpies and Gibbs Free Energies. It is known that accurate knowledge of the enthalpies and the Gibbs free energies are important parameters for determining the thermodynamic properties and kinetics of atmospheric processes. The standard enthalpies of formation ($\Delta H^{\theta}_{f,298}$) of the species, estimated by the group-balanced ismodesmic reactions R4a−R7c, are shown in Table 3. The number and the type of the bonds are conserved in group-balanced ismodesmic reactions. The experimental values[18−21] for $\Delta H^{\theta}_{f,298}$ involved in the ismodesmic reactions are shown as follows: CF_3CF_3, −320.89 kcal/mol; $CF_3CH_2CF_3$, −336.5 kcal/mol; CH_2F_2, −107.71 kcal/mol; CH_3, 34.82 kcal/mol; CF_3, −112.40 kcal/mol; CH_3F, −56.0 kcal/mol; CH_3OCH_3, −44.0 kcal/mol; CH_4,

Table 3. Standard Enthalpies of Formation ($\Delta H^{\theta}_{f,298}$) (kcal/mol) for the Species $(CF_3)_2CFOCH_3$, $(CF_3)_2CFOCH_2$, $(CF_3)_2CFOCHO$, and $(CF_3)_2CFOCO$ at the CCSD(T)//B3LYP/6-311+G(d,p) and QCISD(T)//B3LYP/6-311+G(d,p) Levels

		CCSD(T)//B3LYP		QCISD(T)//B3LYP	
species	isodesmic reaction	$\Delta H^{\theta}_{f,298}$	average	$\Delta H^{\theta}_{f,298}$	average
$(CF_3)_2CFOCH_3$	R4a	−414.07	−411.97	−414.12	−412.08
	R4b	−410.52		−410.64	
	R4c	−411.32		−411.47	
$(CF_3)_2CFOCH_2$	R5a	−361.44	−360.98	−361.56	−361.10
	R5b	−362.83		−362.89	
	R5c	−358.67		−358.85	
$(CF_3)_2CFOCHO$	R6a	−442.90	−443.55	−442.94	−443.55
	R6b	−445.65		−445.60	
	R6c	−442.10		−442.11	
$(CF_3)_2CFOCO$	R7a	−393.85	−396.17	−394.09	−396.34
	R7b	−396.63		−396.80	
	R7c	−398.02		−398.12	

DOI: 10.1021/jp5125553
J. Phys. Chem. A 2015, 119, 1256−1266

−17.89 kcal/mol; CHF_3, −166.60 kcal/mol; and $CHFCF_3$, −166.5 kcal/mol. The standard enthalpies of formation are obtained at the B3LYP/6-311+G(d,p) level and further refined by using the CCSD(T) and QCISD(T) methods on the basis of the B3LYP geometries. From Table 3, the $\Delta H^{\theta}_{f,298}$ values of $(CF_3)_2CFOCH_3$, $(CF_3)_2CFOCH_2$, $(CF_3)_2CFOCHO$, and $(CF_3)_2CFOCO$ are −411.97, −443.55, −360.98, and −396.17 kcal/mol at the CCSD(T)//B3LYP/6-311+G(d,p) level, respectively, which are very close to the results of the QCISD(T)//B3LYP/6-311+G(d,p) level. According to the computational results, the values of $\Delta H^{\theta}_{f,298}$ for $(CF_3)_2CFOCH_3$, $(CF_3)_2CFOCH_2$, $(CF_3)_2CFOCHO$, and $(CF_3)_2CFOCO$ are recommended to be (412.32 ± 1.80), (360.78 ± 2.11), (443.88 ± 1.78), and (395.99 ± 2.14) kcal/mol, respectively.

Reaction enthalpies ($\Delta H^{\theta}_{r,298}$) and reaction Gibbs free energies ($\Delta G^{\theta}_{r,298}$) for all title reactions calculated at the B3LYP/6-311+G(d,p) level, and further refinement by CCSD(T) and QCISD(T) theories, are listed in Table 4. It can be seen from the data in Table 4 that all three reactions are exothermic and spontaneous. The values of $\Delta H^{\theta}_{r,298}$ obtained at the CCSD(T) and QCISD(T) levels are within a very small difference. Similar circumstance can be found regarding $\Delta G^{\theta}_{r,298}$. To compare the reaction enthalpies and reaction Gibbs free energies of the R1 and R2, R1 is more exothermic and spontaneous than R2. Besides all of the above, the calculated bond dissociation energy (D^{θ}_{298}) of the C−H in molecules $(CF_3)_2CFOCH_3$ and $(CF_3)_2CFOCHO$ along with the experimental data are also listed in Table 4. Computed values of 96.9 (97.0) kcal/mol for $(CF_3)_2CFOCH_3$ at the QCISD(T)//B3LYP/6-311+G(d,p) (CCSD(T)//B3LYP) levels are in line with the experimental value within a factor of 2.8−2.9%.[48] It is clear from Table 4 that the C−H values of D^{θ}_{298} in molecule $(CF_3)_2CFOCH_3$ are smaller than that in $(CF_3)_2CFOCHO$, indicating that the H atom of $(CF_3)_2CFOCHO$ is more difficult to abstract than the H atom of $(CF_3)_2CFOCH_3$. This result further proved the above view that the barrier height of R3 is higher than that of R2.

Table 4. Reaction Enthalpies ($\Delta H^{\theta}_{r,298}$) and Reaction Gibbs Free Energies ($\Delta G^{\theta}_{r,298}$) for R1−R3 at the B3LYP/6-311+G(d,p), CCSD(T)//B3LYP/6-311+G(d,p), and QCISD(T)//B3LYP/6-311+G(d,p) Levels (kcal/mol) with the ZPE or TZPE (Thermal Corrections to Enthalpy) Corrections and the Calculated Bond Dissociation Energy (D^{θ}_{298}) of the C−H in molecules $(CF_3)_2CFOCH_3$ and $(CF_3)_2CFOCHO$ along with the Experimental Data (kcal/mol)[a]

		B3LYP	CCSD(T)//B3LYP	QCISD(T)//B3LYP
$\Delta H^{\theta}_{r,298}$	R1	−17.19	−15.52	−15.61
	R2	−2.47	−0.04	−0.09
	R3	−5.21	−3.65	−3.86
$\Delta G^{\theta}_{r,298}$	R1	−18.33	−16.66	−16.75
	R2	−4.84	−2.42	−2.46
	R3	−7.60	−6.04	−6.25
D^{θ}_{298}	$(CF_3)_2CFOCH_3 \rightarrow (CF_3)_2CFOCH_2 + H$	97.0 (99.8)		96.9 (99.8)
	$(CF_3)_2CFOCHO \rightarrow (CF_3)_2CFOCO + H$	99.6		99.8

[a]Experimental values in parentheses are taken from ref 48.

3.3. Properties of Reaction Paths. Panels a and b of Figure 3 depict plots of the classical potential energy curve (V_{MEP}), ground-state vibrational adiabatic energy curve (V^G_a), and zero-point energy (ZPE) curve as a function of s (amu$^{1/2}$ bohr) at the QCISD(T)//B3LYP/6-311+G(d,p) level for reaction channels R1b and R3, respectively, where $V^G_a = V_{MEP}$ + ZPE. It can be seen that the curve of V^G_a is almost similar in shape and that the locations of maximum data correspond with the plot of V_{MEP}; in addition, the ZPE curve has a normal drop near the saddle point for reaction R1b. Therefore, the variational effect is small for the dynamic computation of the channel R1b. In a paper studying the reaction of CF_3OCH_3 with the OH radical by Wu et al.,[22] the V^G_a and V_{MEP} curves are also similar in shape and the maximum values of the two curves are located at the same position (s = 0), which further supports the credibility of our results. As can be seen from Figure 3b, the ZPE is practically constant as s varies, with only a gentle drop near the saddle point. The locations of the maximum values of the two curves are similar in shape; the V^G_a and V_{MEP} curves have little difference in the locations, which indicates that the variational effect has little influence in the calculation of rate constants. A similar conclusion about the size of the variational effect can be obtained in the reaction of CF_3CH_2OCHO with Cl atom by Liu et al.[23] The kinetics study will support the above view.

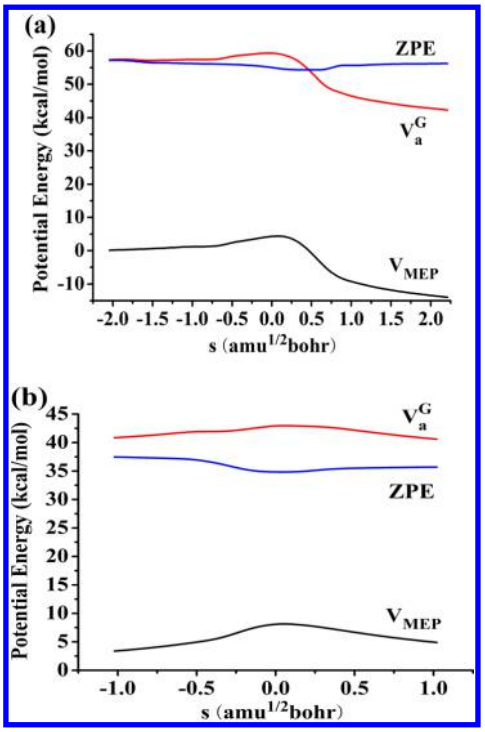

Figure 3. Classical potential energy curve (V_{MEP}), ground-state vibrational adiabatic energy curve (V^G_a), and zero-point energy (ZPE) curve as functions of s (amu$^{1/2}$ bohr) at the QCISD(T)//B3LYP/6-311+G(d,p) level for the reaction channels R1b (a) and R3 (b).

Panels a and b of Figure 4 show that the variations of the generalized normal-mode vibrational frequencies along with the MEPs for the reaction pathways R1b and R3, respectively. It is obvious from Figure 4a that the frequency of mode 1, connecting the stretching vibrational mode of breaking and

DOI: 10.1021/jp5125553
J. Phys. Chem. A 2015, 119, 1256−1266

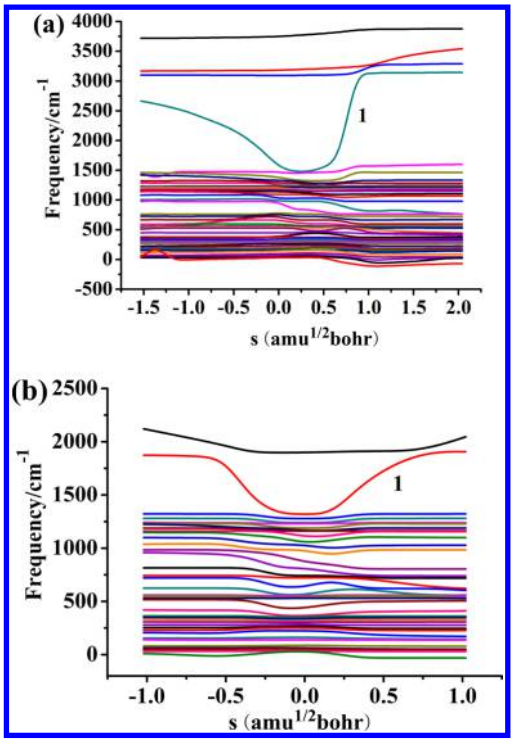

Figure 4. Changes of generalized normal-mode vibrational frequencies as a function of s (amu$^{1/2}$ bohr) at the QCISD(T)//B3LYP/6-311+G(d,p) level for reaction R1b via TS1b (a) and R3 via TS3 (b).

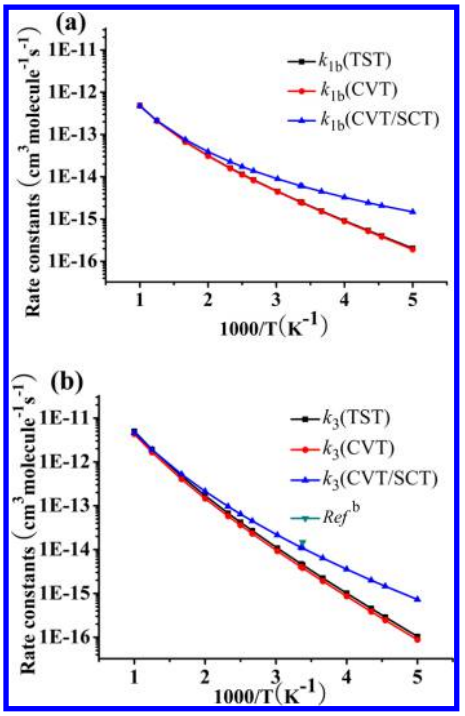

Figure 5. Calculated TST, CVT, and CVT/SCT rate constants as a function of $10^3/T$ for reaction channels R1b (a) and R3 (b) in the temperature range of 200−1000 K.

forming bonds, changes significantly near the saddle point (s = 0). At about s = −1.5 amu$^{1/2}$ bohr, the frequencies represent the region of reactant complex, ER1b, and in the product region associated at about 2.0 amu$^{1/2}$ bohr, the frequencies are associated with the product complex, EP1b. In the variety of the TS, there are 44 vibrational frequencies. The deep minimum in frequency takes place in the range from −0.18 to 0.18 amu$^{1/2}$ bohr, which is known to be the typical behavior of H-transfer reactions. We used to call the significant changes "reaction mode". In Figure 4b, the response of the reaction mode is similar to that given in Figure 4a, and the main regions of s for R3 are from −0.34 to 0.17 amu$^{1/2}$ bohr.

3.4. Rate Constant Calculations. Dual-level dynamics calculations for reactions of $(CF_3)_2CFOCH_3$ + OH/Cl and $(CF_3)_2CFOCHO$ + Cl are carried out using the VTST with the ISPE (VTST-ISPE) method. The PES information on all the reaction pathways, obtained at the QCISD(T)//B3LYP/6-311+G(d,p) level, is put into the POLYRATE version 9.7 program to compute the rate constants over the temperature range of 200−1000 K. The TST, CVT, and CVT/SCT rate constants of the pathways of R1b and R3 are presented in panels a and b of Figure 5, respectively. The variational effect is defined as the ratio between the CVT and TST rate constant, and the tunneling effect is the ratio between the CVT/SCT and CVT rate constant. Figure 5a shows that the rate constants of TST and CVT curves are nearly the same over the whole temperature region (200−1000 K), indicating that variational effect is almost nonexistent and negligible. However, the curves of CVT and CVT/SCT are separated when below 600 K, then similar when the temperature is high. For instance, the specific values of the $k^{CVT/SCT}/k^{CVT}$ are 7.75, 2.48, 1.26, and 0.98, at 200, 296, 500, and 1000 K, respectively. These results suggest that the tunneling effect is significant in low temperatures and then becomes unimportant and insignificant when the temperature is high in the rate constant calculations. Similar phenomenon can be found in other homologous species reactions with OH radical.[20,21,25−27]

Figure 5b demonstrates that the tunneling effect plays an important role in low temperatures and can be omitted in the high-temperature range for R3. For example, the ratios between the $k^{CVT/SCT}$ and the k^{CVT} are 8.24 at 200 K, 2.84 at 296 K, 1.45 at 500 K, and 1.08 at 1000 K. The ratio between the CVT rate constant and TST rate constant is about 0.85 in the temperature range of 200−1000 K, which indicates that the variational effect is so small that it can be ignored. The computed rate constant of 1.08×10^{-14} cm^3 molecule^{-1} s^{-1} is consistent with the experimental data $(1.47 \pm 0.56) \times 10^{-14}$ cm^3 molecule^{-1} s^{-1} at 296 K.

3.5. Branching Ratios and Comparison with Similar Reactions. The calculated rate coefficients of R1a and R1b, and the sum of k_{1a}+ k_{1b}, the total rate constant k_1, along with the corresponding experimental values are plotted in Figure 6. In addition, calculated rate coefficients of R1a and R1b, the total rate constant k_1, and the total rate constant associated with the channel R2 along with the corresponding experimental values are described in Table 5. From Figure 6 and Table 5, it is pleasing to see that the calculated rate constants are in line with the available experimental values within a very small factor. For example, calculated rate constants 1.22×10^{-14} and 1.30×10^{-13} cm^3 molecule^{-1} s^{-1} are in reasonable agreement with the corresponding experimental values of $(1.55 \pm 0.24) \times 10^{-14}$ and $(1.80 \pm 0.42) \times 10^{-13}$ cm^3 molecule^{-1} s^{-1} at 296 K, respectively. The total rate constants and individual rate coefficients increase with temperature rise in the whole temperature range (200−1000 K), which is consistent the reports regarding the investigation of temperature effect of some similar species reactions with OH radical and Cl atom.[15−27]

DOI: 10.1021/jp5125553
J. Phys. Chem. A 2015, 119, 1256−1266

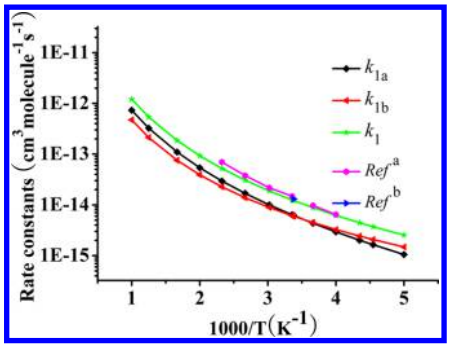

Figure 6. Calculated rate constants k_{1a} and k_{1b} for the individual reaction pathways R1a and R1b, respectively, and the total rate constant k_1 obtained at the QCISD(T)//B3LYP/6-311+G(d,p) level together with the experiment data as a function of $10^3/T$ in the temperature range of 200−1000 K.

From Table 5, it is seen that the overall rate constant of $(CF_3)_2CFOCH_3$ with OH radical is 1 order of magnitude lower than that of reaction $(CF_3)_2CFOCH_3$ + Cl, consistent with the previous experimental investigation.[9] Hence, the H-abstraction reaction with Cl atom is a more important degradation channel for $(CF_3)_2CFOCH_3$ than for that with OH radical. To further understand the title reactions, it is worthwhile to compare the dynamics between the title reactions and similar systems (Cl atom or OH radical with $(CF_3)_2CHOCH_3$, $CF_3CHFOCH_3$, $CF_3CH_2OCH_3$, and CF_3CH_2OCHO).[21,23,27,49−51] In fact, the fluorine and $-CF_3$ group substitution can decrease the reactivity trend. It is interesting to note that the OH radical with some HFEs in rate constants are in this order: $kCF_3CH_2OCH_3$ > $k(CF_3)_2CHOCH_3$ > $kCF_3CHFOCH_3$ > $k(CF_3)_2CFOCH_3$.[21,27,49] From the above comparison, the results suggest that $-CF_3$ group substitution results in a greater decrease than F-substitution in the reactivity trend. With Cl + HFEs as criterion, $kCF_3CH_2OCH_3$ > $kCF_3CHFOCH_3$ > $k(CF_3)_2CFOCH_3$.[50,51] When the calculated overall rate constant of reaction $(CF_3)_2CFOCHO$ + Cl (1.12×10^{-14} cm^3 molecule^{-1} s^{-1}) is compared with that of reaction CF_3CH_2OCHO + Cl (6.43×10^{-14} cm^3 molecule^{-1} s^{-1}) at 298 K,[23] a similar conclusion can be reached.

To further study the mechanism and the products ratios of H-abstraction reaction $(CF_3)_2CFOCH_3$ with OH radical, the temperature dependence of the k_{1a}/k_1 and k_{1b}/k_1 branching ratios are exhibited in Figure 7. From Figure 7, it is evident that

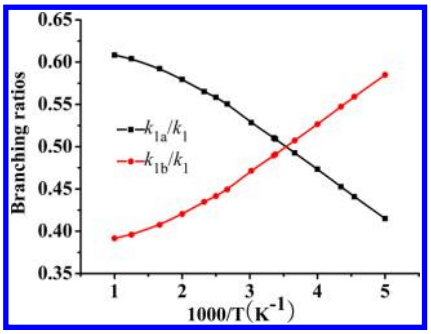

Figure 7. Calculated branching ratios for reaction $(CF_3)_2CFOCH_3$ + OH as a function of $10^3/T$ at the QCISD(T)//B3LYP/6-311+G(d,p) level.

R1b is main channel when the temperature is below about 285 K and then is less competitive than the channel R1a. In a manner of speaking, both of the above paths of H-abstraction are important. For instance, the k_{1a}/k_1 fractions are 41.50%, 50.90%, 57.96%, and 60.83% at 200, 296, 500, and 1000 K, respectively. However, the k_{1b}/k_1 fractions are 58.50% at 200, 49.09% at 296, 42.04% at 500, and 39.17% at 1000 K.

To offer further information concerning reactions R1, R2, and R3, the three-parameter fits based on the calculated rate constants at the QCISD(T)//B3LYP/6-311+G(d,p) level within 200−1000 K give expressions as follows (in units of cm^3 molecule^{-1} s^{-1}):

$$k_1(T) = 1.08 \times 10^{-22} T^{3.38} \exp(-213.31/T)$$

Table 5. Calculated CVT/SCT Rate Constants (cm^3 molecule^{-1} s^{-1}) along with the Experimental Values (in Italics) for Reactions $(CF_3)_2CFOCH_3$ + OH/Cl in the Experimental Temperature Range of 200−500 K

T (K)	k_{1a}	k_{1b}	k_1	k_2
200	1.05×10^{-15}	1.48×10^{-15}	2.53×10^{-15}	2.18×10^{-14}
220	1.64×10^{-15}	2.08×10^{-15}	3.72×10^{-15}	3.38×10^{-14}
230	2.01×10^{-15}	2.43×10^{-15}	4.44×10^{-15}	4.15×10^{-14}
250	2.94×10^{-15}	3.27×10^{-15}	6.21×10^{-15}	6.07×10^{-14}
			$(6.55 \pm 0.37) \times 10^{-15}$[a]	
273	4.35×10^{-15}	4.48×10^{-15}	8.83×10^{-15}	9.04×10^{-14}
			$(9.44 \pm 0.44) \times 10^{-15}$[a]	
296	6.20×10^{-15}	5.98×10^{-15}	1.22×10^{-14}	1.30×10^{-13}
			$(1.55 \pm 0.24) \times 10^{-14}$[b]	*$(1.80 \pm 0.42) \times 10^{-13}$*[b]
298	6.38×10^{-15}	6.12×10^{-15}	1.25×10^{-14}	1.34×10^{-13}
			$(1.45 \pm 0.06) \times 10^{-14}$[a]	
331	1.00×10^{-14}	8.92×10^{-15}	1.89×10^{-14}	2.12×10^{-13}
			$(2.27 \pm 0.09) \times 10^{-14}$[a]	
375	1.69×10^{-14}	1.38×10^{-14}	3.07×10^{-14}	3.62×10^{-13}
			$(3.88 \pm 0.11) \times 10^{-14}$[a]	
400	2.20×10^{-14}	1.74×10^{-14}	3.94×10^{-14}	4.76×10^{-13}
430	2.95×10^{-14}	2.27×10^{-14}	5.22×10^{-14}	6.44×10^{-13}
			$(7.11 \pm 0.18) \times 10^{-14}$[a]	
500	5.39×10^{-14}	3.91×10^{-14}	9.30×10^{-14}	1.20×10^{-12}

[a]Ref 14. [b]Ref 9.

DOI: 10.1021/jp5125553
J. Phys. Chem. A 2015, 119, 1256−1266

$$k_2(T) = 3.55 \times 10^{-22} T^{3.61} \exp(-240.26/T)$$

$$k_3(T) = 3.00 \times 10^{-19} T^{2.58} \exp(-1294.34/T)$$

4. CONCLUSIONS

Reactions $(CF_3)_2CFOCH_3$ + OH/Cl and $(CF_3)_2CFOCHO$ + Cl are investigated in kinetics by the dual-level direct method. The PES information is obtained at the QCISD(T)//B3LYP/6-311+G(d,p) and CCSD(T)//B3LYP/6-311+G(d,p) levels. The values of standard enthalpies of formation, (412.32 ± 1.80) kcal/mol for $(CF_3)_2CFOCH_3$, (362.89 ± 2.11) kcal/mol for $(CF_3)_2CFOCH_2$, (443.88 ± 1.78) kcal/mol for $(CF_3)_2CFOCHO$, and (395.99 ± 2.14) kcal/mol for $(CF_3)_2CFOCO$, are acquired through combining the results at the QCISD(T) and CCSD(T) levels based on the B3LYP geometries.

The rate constants of all the title reactions are calculated by CVT incorporating SCT correction. The agreement between theoretical and experiment is excellent. In the temperature range of 200−1000 K, the variational effect is almost nonexistent or negligible. All three total rate constants are positive temperature coefficients. Calculations show that the H-abstraction rate constant from $(CF_3)_2CFOCH_3$ by OH radical is smaller than that by Cl atom. On the basis of mechanistic and kinetics studies, we suggest that the H-abstraction reaction with Cl atom is a more important degradation channel for $(CF_3)_2CFOCH_3$. Although the hydroxyl radical is more abundant than Cl atom in the atmosphere, the atmospheric implications of reaction of $(CF_3)_2CFOCH_3$ with Cl atom can not be neglected. The three-parameter Arrhenius expressions for the title reactions are $k_1 = 1.08 \times 10^{-22} T^{3.38} \exp(-213.31/T)$, $k_2 = 3.55 \times 10^{-22} T^{3.61} \exp(-240.26/T)$, and $k_3 = 3.00 \times 10^{-19} T^{2.58} \exp(-1294.34/T)$ cm^3 $molecule^{-1}$ s^{-1}. We hope the present theoretical study aids the understanding of the title reactions.

■ AUTHOR INFORMATION

Corresponding Author

*Tel.: +86-431-85099963. Fax: +86-431-85099511. E-mail: panxm460@nenu.edu.cn.

Notes

The authors declare no competing financial interest.

■ ACKNOWLEDGMENTS

The authors thank Professor Donald G. Truhlar for providing the POLYRATE, version 9.7 program. We are grateful for financial support from the National Natural Science Foundation of China (21377021) and the Fund of Jilin Provincial Science & Technology Department (20120401). We are extremely thankful for the reviewers' helpful comments.

■ REFERENCES

(1) Andersen, M. P. S.; Nielsen, O. J.; Karpichev, B.; Wallington, T. J.; Sander, S. P. Atmospheric Chemistry of Isoflurane, Desflurane, and Sevoflurane: Kinetics and Mechanisms of Reactions with Chlorine Atoms and OH Radicals and Global Warming Potentials. *J. Phys. Chem. A* **2012**, *116*, 5806−5820.

(2) Mégie, G. From Stratospheric Ozone to Climate Change: Historical Perspective on Precaution and Scientific Responsibility. *Sci. Eng. Ethics* **2006**, *12*, 596−606.

(3) Wallington, T. J.; Guschin, A.; Stein, J. N. N.; Platz, J.; Sehested, J.; Christensen, L. K.; Nielsen, O. J. Atmospheric Chemistry of $CF_3CH_2OCH_2CF_3$: UV Spectra and Kinetic Data for $CF_3CH(\bullet)OCH_2CF_3$ and $CF_3CH(OO\bullet)OCH_2CF_3$ Radicals and Atmospheric Fate of $CF_3CH(O\bullet)OCH_2CF_3$ Radicals. *J. Phys. Chem. A* **1998**, *102*, 1152−1161.

(4) Sekiya, A.; Misaki, S. The Potential of Hydrofluoroethers to Replace CFCs, HCFCs and PFCs. *J. Fluorine Chem.* **2000**, *101*, 215−221.

(5) Talukdar, R. K.; Mellouki, A.; Gierczak, T.; Burkholder, J. B.; McKeen, S. A.; Ravishankara, A. R. Atmospheric Fate of CF_2H_2, CH_3CF_3, CHF_2CF_3, and CH_3CFCl_2: Rate Coefficients for Reactions with OH and UV Absorption Cross Sections of CH_3CFCl_2. *J. Phys. Chem.* **1991**, *95*, 5815−5821.

(6) Ravishankara, A. R.; Turnipseed, A. A.; Jensen, N. R.; Barone, S.; Mills, M.; Howard, C. J.; Solomon, S. Do Hydrofluorocarbons Destroy Stratospheric Ozone? *Science* **1994**, *263*, 71−75.

(7) Atkinson, R.; Aschmann, S. M.; Pitts, J. N. Kinetics of the Reactions of Naphthalene and Biphenyl with OH Radicals and with O_3 at 294 ± 1 K. *Environ. Sci. Technol.* **1984**, *18*, 110−113.

(8) Oyaro, N.; Sellevag, S.; Nlelsen, A. J. Study of the OH and Cl-initiated Oxidation, IR Absorption Cross-Section, Radiative Forcing, and Global Warming Potential of Four C_4-Hydrofluoroethers. *Environ. Sci. Technol.* **2004**, *38*, 5567−5576.

(9) Andersen, L. L.; Østerstrøma, F. F.; Nielsen, O. J.; Andersen, M. P. S.; Wallington, T. J. Atmospheric Chemistry of $(CF_3)_2CFOCH_3$. *Chem. Phys. Lett.* **2014**, *607*, 5−9.

(10) Zhang, M. L.; An, T. C.; Fu, J. M.; Sheng, G. Y.; Wang, X. M.; Hu, X. H.; Ding, X. J. Photocatalytic Degradation of Mixed Gaseous Carbonyl Compounds at Low Level on Adsorptive TiO_2/SiO_2 Photocatalyst Using a Fluidized Bed Reactor. *Chemosphere* **2006**, *64*, 423−431.

(11) Blanco, M. B.; Rivela, C.; Teruel, M. A. Tropospheric Degradation of 2,2,2-Trifluoroethyl Butyrate: Kinetic Study of Their Reactions with OH Radicals and Cl Atoms at 298 K. *Chem. Phys. Lett.* **2013**, *578*, 33−37.

(12) Lestard, M. E. D.; Tuttolomondo, M. E.; Wann, D. A.; Robertson, H. E.; Rankinb, D. H.; Altabef, A. B. Experimental and Theoretical Structure and Vibrational Analysis of Ethyl Trifluoroacetate, $CF_3CO_2CH_2CH_3$. *J. Raman. Spectrosc.* **2010**, *41*, 1357−1368.

(13) Chandra, A. K. Theoretical Studies on the Kinetics and Mechanism of the Gas-Phase Reactions of CHF_2OCHF_2 with OH Radicals. *J. Mol. Model.* **2012**, *18*, 4239−4247.

(14) Tokuhashi, K.; Takahashi, A.; Kaise, M.; Kondo, S.; Sekiya, A.; Yamashita, S.; Ito, H. Rate Constants for the Reactions of OH Radicals with $CH_3OCF_2CF_3$, $CH_3OCF_2CF_2CF_3$, and $CH_3OCF(CF_3)_2$. *Int. J. Chem. Kinet.* **1999**, *31*, 846−853.

(15) Devi, K. J.; Chandra, A. K. Theoretical Investigation of the Gas-Phase Reactions of $(CF_3)_2CHOCH_3$ with OH Radical. *Chem. Phys. Lett.* **2011**, *502*, 23−28.

(16) Singh, H. J.; Gour, N. K.; Rao, P. K.; Tiwari, L. Theoretical Investigation on the Kinetics and Branching Ratio of the Gas Phase Reaction of Sevoflurane with Cl Atom. *J. Mol. Model.* **2013**, *19*, 4815−4822.

(17) Ren, H. J.; Yang, X. H.; Li, X. J.; Liu, Y.; Wei, X. The Hydrogen Abstraction Reaction Mechanism and Rate Constants from 200 to 2000 K Between Sevoflurane and Chlorine Atom: A Theoretical Investigation. *Chem. Phys. Lett.* **2014**, *605−606*, 28−34.

(18) Bai, F. Y.; Sun, Y. Q.; Wang, X.; Jia, Z. M.; Wang, R. S.; Pan, X. M. Theoretical Investigation of the Mechanisms and Dynamics of the Reaction CHF_2OCF_2CHFCl+Cl. *J. Mol. Model.* **2014**, *20*, 2419.

(19) Deka, R. C.; Mishra, B. K. Theoretical Studies on Kinetics, Mechanism and Thermochemistry of Gas-Phase Reactions of HFE-449mec-f with the OH Radicals and Chlorine Atom. *J. Mol. Graphics Modell.* **2014**, *53*, 23−30.

(20) Song, G. C.; Jia, X. J.; Gao, Y.; Luo, J.; Yu, Y. B.; Wang, R. S.; Pan, X. M. Theoretical Studies on the Mechanisms and Dynamics of OH Radicals with $CH_2FCF_2OCHF_2$ and CH_2FOCH_2F. *J. Phys. Chem. A* **2010**, *114*, 9057−9068.

(21) Sun, H.; Gong, H. W.; Pan, X. M.; Hao, L. Z.; Sun, C. C.; Wang, R. S.; Huang, X. R. Theoretical Investigation of the Reaction of

DOI: 10.1021/jp5125553
J. Phys. Chem. A 2015, 119, 1256−1266

$CF_3CHFOCH_3$ with OH Radical. *J. Phys. Chem. A* **2009**, *113*, 5951−5957.
(22) Wu, J. Y.; Liu, J. L.; Li, Z. S.; Sun, C. C. Theoretical Study of the Reaction of CF_3OCHF_2 with the Hydroxyl Radical and the Chlorine Atom. *ChemPhysChem* **2004**, *5*, 1336−1344.
(23) Liu, H. X.; Liu, Y. C.; Wan, S. Q.; Liu, J. Y. Reaction of Cl with CF_3CH_2OCHO: A Mechanistic and Kinetic Study. *J. Mol. Struct.: THEOCHEM* **2010**, *944*, 124−131.
(24) Chen, L.; Kutsuna, S.; Tokuhashi, K.; Sekiya, A.; Tamai, R.; Hibino, Y. Kinetics and Mechanism of $(CF_3)_2CHOCH_3$ Reaction with OH Radicals in an Environmental Reaction Chamber. *J. Phys. Chem. A* **2005**, *109*, 4766−4771.
(25) Yang, L.; Liu, J. L.; Wang, L.; He, H. Q.; Wang, Y.; Li, Z. S. Theoretical Study of the Reaction of $CF_3CH_2OCHF_2$+OH/Cl and Its Product Radicals and Parent Ether ($CH_3CH_2OCH_3$) with OH. *J. Comput. Chem.* **2008**, *29*, 550−561.
(26) Yang, L.; Liu, J. L.; Wan, S. Q.; Li, Z. S. Theoretical Studies of the Reactions of $CF_3CHClOCHF_2$/$CF_3CHFOCHF_2$ with OH Radical and Cl Atom and Their Product Radicals with OH. *J. Comput. Chem.* **2009**, *30*, 565−580.
(27) Mishra, B. K.; Lily, M.; Chakrabartty, A. K.; Bhattacharjee, D.; Deka, R. C.; Chandra, A. K. Theoretical Investigation of Atmospheric Chemistry of Volatile Anaesthetic Sevoflurane: Reactions with the OH Radicals and Atmospheric Fate of the Alkoxy Radical $(CF_3)_2CHOCHFO$: Thermal Decomposition vs. Oxidation. *New J. Chem.* **2014**, *38*, 2813−2822.
(28) Becke, A. D. A New Mixing of Hartree−Fock and Local Density-Functional Theories. *J. Chem. Phys.* **1993**, *98*, 1372−1377.
(29) Lee, C.; Yang, W.; Parr, R. G. Development of the Colle-Salvetti Correlation-Energy Formula into a Functional of the Electron Density. *Phys. Rev. B: Condens. Matter Mater. Phys.* **1999**, *37*, 785−789.
(30) Tang, Y. Z.; Pan, Y. R.; Sun, J. Y.; Wang, R. S. Ab Initio/DFT Theory and Multichannel RRKM Study on the Mechanisms and Kinetics for the CH_3S + CO Reaction. *Chem. Phys.* **2008**, *344*, 221−226.
(31) Fan, X. W.; Ju, X. H. Theoretical Studies on Four-Membered Ring Compounds with NF_2, ONO_2, N_3, and NO_2 Groups. *J. Comput. Chem.* **2008**, *29*, 505−513.
(32) Gonzalez, C.; Schlegel, H. B. An Improved Algorithm for Reaction Path Following. *J. Chem. Phys.* **1989**, *90*, 2154−2161.
(33) Gonzalez, C.; Schlegel, H. B. Reaction Path Following in Mass-Weighted Internal Coordinates. *J. Chem. Phys.* **1990**, *94*, 5523−5527.
(34) Raghavachari, K.; Trucks, G. W.; Pople, J. A.; Head-Gordon, M. A. A Fifth-Order Perturbation Comparison of Electron Correlation Theories. *Chem. Phys. Lett.* **1989**, *157*, 479−483.
(35) People, J. A.; Head-Gordon, M. A.; Raghavachari, K. Quadratic Configuration Interaction. A General Technique for Determining Electron Correlation Energies. *J. Chem. Phys.* **1989**, *87*, 5968−5975.
(36) Zhang, Y. J.; Chao, K.; Sun, J. Y.; Zhang, W. Q.; Shi, H. J.; Yao, C.; Su, Z. M.; Pan, X. M.; Zhang, J. P.; Wang, R. S. Theoretical Study on the Gas Phase Reaction of Allyl Chloride with Hydroxyl Radical. *J. Chem. Phys.* **2014**, *140*, 084309(1−11).
(37) Frisch, M. J.; Trucks, G. W.; Schlegel, H. B.; Scuseria, G. E.; Robb, M. A.; Cheeseman, J. R.; Montgomery, et al. *Gaussian 09*; Gaussian, Inc.: Wallingford, CT, 2010.
(38) Garrett, B. C.; Truhlar, D. G. Criterion of Minimum State Density in the Transition State Theory of Bimolecular Reactions. *J. Chem. Phys.* **1979**, *70*, 1593−1598.
(39) Garrett, B. C.; Truhlar, D. G. Generalized Transition State Theory. Bond Energy-Bond Order Method for Canonical Variational Calculations with Application to Hydrogen Atom Transfer Reactions. *J. Am. Chem. Soc.* **1979**, *101*, 4534−4548.
(40) Garrett, B. C.; Truhlar, D. G.; Grev, R. S.; Magnuson, A. W. Improved Treatment of Threshold Contributions in Variational Transition-State Theory. *J. Phys. Chem.* **1980**, *84*, 1730−1748.
(41) Lu, D. H.; Truong, T. N.; Melissas, V. S.; Lynch, G. C.; Liu, Y. P.; Grarrett, B. C.; Steckler, R.; Issacson, A. D.; Rai, S. N.; Hancock, G. C.; Lauderdale, J. G.; Joseph, T.; Truhlar, D. G. A New Version of a Computer Program for the Calculation of Chemical Reaction Rates for Polyatomics. *Comput. Phys. Commun.* **1992**, *71*, 235−262.
(42) Liu, Y. P.; Lynch, G. C.; Truong, T. N.; Lu, D. H.; Truhlar, D. G.; Garrett, B. C. Molecular Modeling of the Kinetic Isotope Effect for the [1,5]-Sigmatropic Rearrangement of Cis-1,3-Pentadiene. *J. Am. Chem. Soc.* **1993**, *115*, 2408−2415.
(43) Chuang, Y. Y.; Corchado, J. C.; Truhlar, D. G. Mapped Interpolation Scheme for Single-Point Energy Corrections in Reaction Rate Calculations and a Critical Evaluation of Dual-Level Reaction Path Dynamics Methods. *J. Phys. Chem. A* **1999**, *103*, 1140−1149.
(44) Corchado, J. C.; Chuang, Y. Y.; Fast, P. L.; Hu, W. P.; Liu, Y. P.; Lynch, G. C.; Nguyen, K. A.; Jackels, C. F.; Fernandez-Ramos, A.; Ellingson, B. A. et al. *POLYRATE*, version 9.7; University of Minnesota: Minneapolis, MN, 2007.
(45) Ignatyev, I. S.; Xie, Y. M.; Allen, W. D.; Schaefer, H. F. Mechanism of the C_2H_5+O_2 Reaction. *J. Chem. Phys.* **1997**, *107*, 141−155.
(46) Schlegel, H. B.; Sosa, C. Ab Initio Molecular Orbital Calculations on Atomic Fluorine + Molecular Hydrogen → Hydrogen Fluoride + Atomic Hydrogen and Hydroxyl + Molecular Hydrogen → Water + Atomic Hydrogen Using Unrestricted Moeller-Plesset Perturbation Theory with Spin Projection. *Chem. Phys. Lett.* **1988**, *145*, 329−333.
(47) Jia, X. J.; Liu, Y. J.; Sun, J. Y.; Sun, H.; Su, Z. M.; Pan, X. M.; Wang, R. S. Theoretical Investigation of the Reactions of $CF_3CHFOCF_3$ with the OH Radical and Cl Atom. *J. Phys. Chem. A* **2010**, *114*, 417−424.
(48) Chandra, A. K.; Uchimaru, T.; Urata, S.; Sugie, M.; Sekiya, A. Estimation of Rate Constants for Hydrogen Atom Abstraction by OH Radicals Using the C-H Bond Dissociation Enthalpies: Haloalkanes and Haloethers. *Int. J. Chem. Kinet.* **2003**, *35*, 130−138.
(49) Mishra, B. K.; Lily, M.; Deka, R. C.; Chandra, A. K. Theoretical Investigation on Gas-Phase Reaction of $CF_3CH_2OCH_3$ with OH Radicals and Fate of Alkoxy Radicals $(CF_3CH(O\bullet)OCH_3$/$CF_3CH_2OCH_2O\bullet$. *J. Mol. Graphics Modell.* **2014**, *50*, 90−99.
(50) Liu, F. Y.; Long, Z. W.; Tan, X. F.; Long, B. The Reaction Mechanisms and Kinetics of $CF_3CHFOCH_3$ and $CHF_2CHFOCF_3$ with Atomic Chlorine: A Computational Study. *J. Mol. Model.* **2014**, *20*, 2435.
(51) Zhang, H.; Liu, C.; Y; Zhang, G. L.; Hou, W. J.; Sun, M.; Liu, B.; Li, Z. S. Theoretical Studies of the Reactions of Cl Atoms with $CF_3CH_2OCH_nF_{(3-n)}$ (n = 1, 2, 3). *Theor. Chem. Acc.* **2010**, *127*, 551−560.

DOI: 10.1021/jp5125553
J. Phys. Chem. A 2015, 119, 1256−1266